

IMTS-Mixer: Mixer-Networks for Irregular Multivariate Time Series Forecasting

Christian Klötergens
University of Hildesheim
ISMLL
Hildesheim, Germany
kloetergens@ismll.de

Tim Dervedde
University of Hildesheim
ISMLL
Hildesheim, Germany
dervedde@ismll.de

Lars Schmidt-Thieme
University of Hildesheim
ISMLL
Hildesheim, Germany
schmidt-thieme@ismll.de

Abstract

Forecasting Irregular Multivariate Time Series (IMTS) has recently emerged as a distinct research field, necessitating specialized models to address its unique challenges. While most forecasting literature assumes regularly spaced observations without missing values, many real-world datasets—particularly in healthcare, climate research, and biomechanics—violate these assumptions. Time Series (TS)-mixer models have achieved remarkable success in regular multivariate time series forecasting. However, they remain unexplored for IMTS due to their requirement for complete and evenly spaced observations. To bridge this gap, we introduce IMTS-Mixer, a novel forecasting architecture designed specifically for IMTS. Our approach retains the core principles of TS mixer models while introducing innovative methods to transform IMTS into fixed-size matrix representations, enabling their seamless integration with mixer modules. We evaluate IMTS-Mixer on a benchmark of four real-world datasets from various domains. Our results demonstrate that IMTS-Mixer establishes a new state-of-the-art in forecasting accuracy while also improving computational efficiency.

CCS Concepts

• Computing methodologies → Supervised learning.

Keywords

Irregular Multivariate Time Series Forecasting

ACM Reference Format:

Christian Klötergens, Tim Dervedde, and Lars Schmidt-Thieme. 2025. IMTS-Mixer: Mixer-Networks for Irregular Multivariate Time Series Forecasting. In . ACM, New York, NY, USA, 10 pages. <https://doi.org/10.1145/nnnnnnn>.

1 Introduction

Time series forecasting plays a pivotal role in numerous fields such as economics, climate science, healthcare and more. As of today, a vast majority of the proposed models in the statistics and machine learning literature assume that all variables are observed at the same regular interval. However, this assumption does not hold in a

multitude of applications in various fields. In such cases, models need to be able to predict the future development of variables that are observed in irregular patterns. When time series encompass multiple variables (channels), which are observed irregularly we refer to them as **Irregular Multivariate Time Series (IMTS)**. An IMTS is typically considered to have missing values because most channels are not observed simultaneously. Hence, at a single observation time point the states of only few channels are known, while the states of the remaining channels are unknown (missing), as illustrated in Figure 1. IMTS without missing values are uncommon, as it would require an observation mechanism that can access all channels at every observation step but is somehow disabled to sample observations in a regular pattern. Therefore, we define IMTS with missing values as the default scenario that generalizes the rare special case of IMTS without missing values.

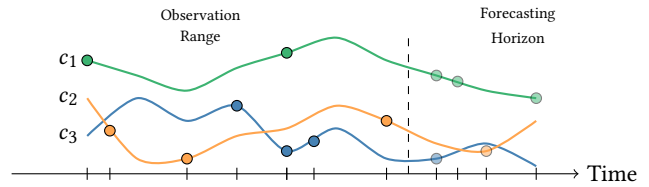


Figure 1: Example for an IMTS Forecasting Task. The observations and forecasting targets are irregularly spaced.

Previous studies [2, 27, 32] have demonstrated the necessity of specifically designed IMTS forecasting models as regular time series forecasting models perform poorly when applied to IMTS.

Initially, researchers proposed models based on Ordinary Differential Equations (ODEs) [1, 3, 5, 17]. ODEs are intuitively well-suited for IMTS modeling, because they are used in various scientific fields such as Physics, Chemistry and Biology to model complex dynamics in a continuous manner. However, learning an ODE that is defined by a neural network (Neural ODE [3]) has shown to be ineffective. Furthermore, ODE-based models typically need a computationally expensive ODE-solver, which results in slow training and inference.

More recent architectures encode IMTS into graphs [27, 32] and provide a significant lift over ODE-based models in terms of forecasting accuracy and computational efficiency.

On the other hand, time series mixer (TS-mixer) models [4, 7] are the state-of-the-art models for regular multivariate time series (RMTS) forecasting, making it intriguing to apply that approach to IMTS. However, TS-Mixer treats a time series as fixed-size matrix and applies fully connected layers along the time and channel dimension without modeling observation times explicitly. Hence,

Permission to make digital or hard copies of all or part of this work for personal or classroom use is granted without fee provided that copies are not made or distributed for profit or commercial advantage and that copies bear this notice and the full citation on the first page. Copyrights for components of this work owned by others than the author(s) must be honored. Abstracting with credit is permitted. To copy otherwise, or republish, to post on servers or to redistribute to lists, requires prior specific permission and/or a fee. Request permissions from permissions@acm.org.
Conference'17, Washington, DC, USA

© 2025 Copyright held by the owner/author(s). Publication rights licensed to ACM.
ACM ISBN 978-x-xxxx-xxxx-x/YYYY/MM
<https://doi.org/10.1145/nnnnnnn>

TS-Mixer is not applicable to IMTS out-of-the-box. Instead, it is necessary to transform each channel into a fixed-size vector, resulting in a fixed-size matrix when these channel-vectors are stacked.

In this work, we introduce IMTS-Mixer, a new architecture for IMTS forecasting. In order to apply mixer networks to IMTS, we implement a novel aggregation method that encodes an irregularly observed channel into a fixed-sized vector. For every channel, we embed each observation into a vector and aggregate these vectors with a convex sum. The weights for the convex sums are inferred based on observation times and the observed values. We yield one vector per channel and combine these channels into a matrix which we can feed into mixer-blocks to capture intra- and inter-channel dependencies. Finally, we introduce a novel module to predict IMTS forecasting targets from the channel embeddings.

To evaluate the performance of IMTS-Mixer, we conduct experiments on the evaluation tasks proposed by Zhang et al. [32]. Our results show that IMTS-Mixer yields the most accurate forecasts on three out of four evaluation tasks. On the fourth task, we establish a new state-of-the-art by evaluating an additional model (GraFITi [27]) on the benchmark.

Hence, the findings of this work have a profound impact on both researchers and practitioners in the field of IMTS forecasting. Our contributions contain the following:

- We propose IMTS-Mixer, the first IMTS forecasting model, that builds upon TS-mixer [4, 7] a simple, yet effective architecture that is well-established in RMTS forecasting.
- In order to make mixer networks applicable, we introduce a novel encoder that aggregates irregularly observed input channels into fixed-sized vectors.
- We introduce a decoder that can predict IMTS forecasting targets based on fixed-sized vectors.
- Our experiments establish a new state-of-the-art on every evaluation task from the benchmark we used.
- For reproducibility, we share our code on GitHub: <https://anonymous.4open.science/r/IMTS-Mixer-D63C/>

2 Related Work

2.1 RMTS Forecasting

The Regular Multivariate Time Series (RMTS) forecasting literature recently focused on transformer-based [21] architectures [13, 15, 24, 35, 36]. However, Zeng et al. showed that a simple model based on linear layers (DLinear [29]) can be competitive and partially outperform the more complex transformer architectures. Additionally, mixer architectures have been adapted from the computer vision domain [20] to time series [4, 7]. They exclusively rely on fully-connected networks, that are alternately applied along the channel and time dimension and achieve state-of-the-art results.

2.2 IMTS Forecasting

2.2.1 Ordinary Differential Equations. Initially, researchers relied on Neural ODE [3] related approaches to model IMTS [1, 5, 16, 17]. ODEs are the prevalent framework in science and engineering to model how systems evolve over time in a continuous manner. However, using neural networks to represent ODE systems has proven to be less effective than other IMTS modeling approaches and also incurs relatively long inference times [27, 32].

2.2.2 Graph Neural Networks for IMTS forecasting. Apart from the ODE-based approaches the Transformable Patch Graph Neural Network (tPatchGNN) [32] applies a patching mechanism to each channel. The patches are then processed with a Transformer and serve as input for a Graph Neural Network (GNN) that models inter-channel dependencies.

Additionally, we want to highlight Graphs for Forecasting Irregular Multivariate Time Series (GraFITi) [27]. Here, the IMTS is represented with a graph where channels and time points are nodes and observed values are stored in the edges between the corresponding time and channel nodes. Forecasts are made by predicting the edge values of query-time nodes with graph attention layers. While this approach provides state-of-the-art performance it also comes with major drawbacks, that relate to the graph structure itself. GraFITi relies on time nodes that are connected to multiple channel nodes, corresponding to observation steps that observe more than one channel. If only one channel is observed at a time, the resulting graph is disconnected, rendering GraFITi incapable of modeling inter-channel interactions.

Another problem of GraFITi lies in the fact that the query nodes are indirectly connected and hence influence each other. That entails that predictions will change depending on what *other* queries we give to the model.

2.2.3 Multi Time Attention. The Multi Time Attention (mTAN) [18] mechanism imputes an IMTS at predefined reference points, by aggregating the observations within a channel with multi-head attention (MHA) [21] where attention weights are computed only dependent on the observation time. The estimates of these reference points are then further processed by a linear layer and consequently fed into a Recurrent Neural Network (RNN).

The output of this RNN can then either be used to solve IMTS classification or interpolation. IMTS interpolation and forecasting are closely related. The problems only differ in the position of the queries. While interpolation queries lay in between observations, forecasting queries are positioned after the latest observation time. mTAN interpolates by applying the same attention mechanism replacing reference points with query points. The same approach can be followed for IMTS forecasting. Imputing reference points can be interpreted as encoding IMTS channels into vectors where each vector-element corresponds to a reference point. This is closely related to the approach of this work. Furthermore, we also use vector encoding to leverage a module that was originally designed for RMTS, but instead of RNN we rely on TS-mixer.

3 Problem Formulation

Definition 3.1 (IMTS). An Irregularly sampled Multivariate Time Series (IMTS) can be represented as a sequence of C channels $X := (X_1, \dots, X_C) \in \mathcal{X}$. A channel $X_c \in (\mathbb{R} \times \mathbb{R})^*$ is a sequence of observation-tuples: $X_c := ((t_{c,i}, v_{c,i}))_{i=1:N_c}$ of pairs where:

- $t_{c,i} \in \mathbb{R}$ is the time of observation
- $v_{c,i} \in \mathbb{R}$ is the observed value of channel c at $t_{c,i}$

We use $*$ to indicate the space of sequences.

Definition 3.2 (Query). Analogous to the definition of IMTS, we define a forecasting query as the sequence of C channel specific

queries: $Q := (Q_1, \dots, Q_C) \in \mathcal{Q}$, with $Q_c := (q_{c,i})_{i=1:K_c}$. A query includes the future time points that need to be forecasted. The answer to the queries can be then represented by $Y := (Y_1, \dots, Y_C) \in \mathcal{Y}$, with $Y_c := (y_{c,i})_{i=1:K_c}$, where $y_{c,i}$ corresponds to $q_{i,c}$. Hence, Q_c and Y_c are sequences of equal lengths ($K_c \in \mathbb{N}$).

Problem 1. We define the IMTS forecasting problem as follows: given M triplets $\left((X^{(m)}, Q^{(m)}, Y^{(m)}) \right)_{m=1:M}$ drawn from a distribution ρ and a loss function $\ell : \mathcal{Y} \times \mathcal{Y} \rightarrow \mathbb{R}$, find a model $\hat{Y} : \mathcal{X} \times \mathcal{Q} \rightarrow \mathcal{Y}$, that minimizes the expected loss of predictions and ground truth:

$$\operatorname{argmin}_{\hat{Y}} \mathbb{E}_{\{X, Q, Y\} \sim \rho} [\ell(\hat{Y}(X, Q), Y)]. \quad (1)$$

In this work, we focus on two loss functions for training and evaluation: Mean Squared Error (MSE) and Mean Absolute Error (MAE). In the experiments we refer to implementations defined as follows:

$$\text{MSE}(Y, \hat{Y}) := \frac{1}{\sum_{m=1}^M \sum_{c=1}^C K_c^{(m)}} \sum_{m=1}^M \sum_{c=1}^C \sum_{i=1}^{K_c^{(m)}} (y_{c,i}^{(m)} - \hat{y}_{c,i}^{(m)})^2 \quad (2)$$

$$\text{MAE}(Y, \hat{Y}) := \frac{1}{\sum_{m=1}^M \sum_{c=1}^C K_c^{(m)}} \sum_{m=1}^M \sum_{c=1}^C \sum_{i=1}^{K_c^{(m)}} |y_{c,i}^{(m)} - \hat{y}_{c,i}^{(m)}| \quad (3)$$

Here, $K_c^{(m)}$ refers to the number of queries in an instance's (m) channel (c) and $\hat{y}_{c,i}^{(m)} = \hat{Y}(X^{(m)}, q_{c,i}^{(m)})$. We explicitly define these well-established loss functions to avoid ambiguity, as other variants are theoretically possible. For example one could compute the mean over all queries from an instance or channel and then compute the average of these means. This would prevent instances and channels with an extraordinary number of queries to have a higher weight on the training and evaluation. However, in this work we rely on the loss functions established in the literature [1, 5, 17, 27, 32] and follow the definitions above.

4 Method

Figure 4 depicts an overview over IMTS-Mixer. In the subsections below we explain each module, starting with the channel aggregation method, the key innovation of this work that is depicted in Figure 2. Subsequently, we explain how we apply the mixer blocks to the aggregated channels and how we predict for the query time points.

4.1 Observation-Encoder

To aggregate the observations of a channel in a meaningful way, we first transform observation tuples (v_i, t_i) into higher dimensional vector-embeddings $h_i \in \mathbb{R}^D$. From here on, we will write v_i, t_i for $v_{c,i}, t_{c,i}$, if the channel c is not relevant. First we, encode the scalar value v into the hidden dimension D with a linear layer:

$$v_i^{\text{enc}} = W^{v_{\text{enc}}} v_i + b^{v_{\text{enc}}}, \quad (4)$$

where $W^v \in \mathbb{R}^D$ and $b^v \in \mathbb{R}^D$ are trainable weights and biases. To include information about the observation time, we multiply the encoded observation value element-wise with a vector of the same length that is inferred by feeding the scalar observation time

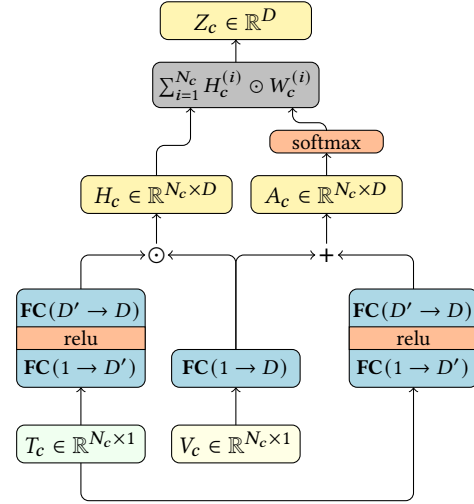


Figure 2: IMTS-Mixer's channel aggregation architecture. For simplicity, we split a channel X_c into the observation times T_c and observed values V_c . For each channel, the aggregation module shown summarizes a varying number of observation tuples into a fixed-sized vector Z_c . We use $\text{FC}(A \rightarrow B)$ to symbolize a single fully connected linear layer with A input and B output neurons.

through a 2-layer fully connected network with relu activation function:

$$t_i^{\text{enc}} = W_2^{t_{\text{enc}}} (\text{relu}(W_1^{t_{\text{enc}}} t_i + b_1^{t_{\text{enc}}})) + b_2^{t_{\text{enc}}} \quad (5)$$

$$h_i = t_i^{\text{enc}} \odot v_i^{\text{enc}} \quad (6)$$

4.2 Channel Aggregation

After embedding each observation into a vector we aggregate the embeddings within a weighted convex sum. The respective weights α_i are based on the observation time and the observed value. Here, we reuse the value-encoding v_i^{enc} that was used to compute the observation embedding and add it to the output of another neural network that inputs time as a scalar.

$$\alpha_i = W_2^{t_{\text{weight}}} (\text{relu}(W_1^{t_{\text{weight}}} t_i + b_1^{t_{\text{weight}}})) + b_2^{t_{\text{weight}}} \quad (7)$$

We aggregate the observations embeddings of each channel to obtain the channel encoding $Z_c \in \mathbb{R}^D$. Specifically Z_c is the encoding of the IMTS channel X_c . While X_c is a set of arbitrary many observation tuples, Z_c is a vector of size D for every channel c . The computation of the weighted convex sum can be expressed with:

$$Z_c = \sum_{i=1}^{N_c} \text{softmax}(A_c)_i \odot h_i \quad (8)$$

Here, $A_c \in \mathbb{R}^{N_c \times D}$ is the matrix created by concatenating the N_c many α_i -vectors as defined by Equation (5), with N_c referring to the number of observations in channel X_c . The softmax function is applied over the rows of A_c to ensure that all weights contained in the vectors α_i are positive and add up to one in each dimension.

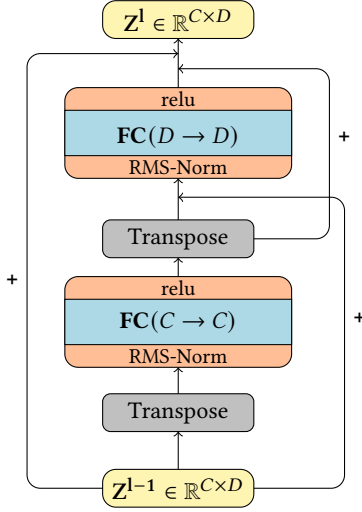


Figure 3: Architecture of the mixer block from IMTS-Mixer. $\text{FC}(A \rightarrow B)$ refers to a linear layer with A input and B output neurons.

4.3 Channel-Bias

The proposed channel encoder shares the weights for all channels and thus only learns to embed them based on the patterns in the observation horizon. To learn channel specific information and distinguish the channel embeddings, we add channel biases $b_c \in \mathbb{R}^D$. The final channel encoding is then computed as

$$Z_c^+ = Z_c + b_c \quad (9)$$

This helps also for the case where a channel is unobserved in the observation horizon. In that case, we define the channel encoding simply to be the bias term of that channel. In Section 6.5 we show an ablation study showing that this is sufficient for encoding the channels and no other channel specific weights are necessary. Note also that the subsequent mixer blocks can learn channel specific patterns as well as mix information across channels.

4.4 Mixer Blocks

Time series mixer networks [4, 7] apply fully connected layers along the time and channel dimension alternately. They are well-established in regular time series forecasting and yield state-of-the-art forecasting despite exclusively relying on vanilla fully connected layers [4, 7].

A mixer network can only be applied to 2-D inputs where both dimensions are fixed across instances. Additionally, it cannot directly process NaN-values. While these conditions are met in regular time series, they can never be satisfied in any IMTS dataset.

However, when we aggregate each channel of an IMTS into fixed-sized vectors as we propose in the previous subsections, we encode an IMTS in matrix form, in which the rows directly represent the channels. As a result, we are able to harness the power of mixer networks to learn channel interactions and extract the information relevant to forecasting.

Instead of using mixer blocks, we could also flatten the hidden state and apply fully connected layers $\mathbb{R}^{CD} \rightarrow \mathbb{R}^{CD}$. However,

the number of parameters $((CD)^2)$ of such a layer would explode. Hence, the resulting model would demand an unnecessary amount of memory while being prone to overfitting.

We define a mixer block as two fully connected layers that are applied subsequently along the hidden dimension D and the input channels C . To learn non-linear dependencies we add relu as an activation function to each layer. Aligning with TS-mixer architectures established in RMTS forecasting [4, 7], we add residual connections as they are known to simplify the optimization while enhancing expressiveness [8]. Furthermore, we also apply normalization before each fully connected layer as it is known to improve learning deep architectures and was also added to RMTS TS-mixer architectures [4, 7]. Specifically, we use Rooted-Mean-Square Layer Normalization (RMS-Norm) [30].

Theoretically, we could vary the hidden dimension D after each layer as well as the number of (latent) channels C . The next channel-to-channel layer would simply have to adjust its input dimension to the output dimension of the previous channel-to-channel layer. However, the final channel-to-channel layer is restricted to have an output dimension of C , due to our method of utilizing the outcome of the mixer blocks for the final prediction. We describe the respective method in the next subsection. We decide to keep the output dimension of channel-to-channel layers as C .

Furthermore, we also keep the hidden dimension at D except for the last layer where we allow us to choose a different output dimension D_{out} . This decision is supposed to account for the fact that the range in which queries are given can significantly vary from the observation time. For example, a model might be tasked to predict a month based on two years. As the mixer blocks are supposed to map a sequence of observations into a latent encoding of an IMTS's state during the forecasting span [4, 7] the output dimension D_{out} should match the necessary complexity. Staying in the given example, the aggregated channels of dimension D need to contain all the relevant information of two years, but the channel representations emitted by the final mixer block only have to encode information that correspond to one month. Therefore, it would be adequate if D_{out} is smaller than D .

IMTS-Mixer contains L mixer blocks, and we define the output of the l^{th} mixer block as:

$$Z'^{(l)} = Z^{(l-1)} + \text{relu}(W_C^{(l)} \text{RMS}(Z^{(l-1)}) + b_C^{(l)}) \quad (10)$$

$$Z^{(l)} = Z^{(l-1)} + Z'^{(l)} + \text{relu}(W_D^{(l)} \text{RMS}(Z'^{(l)}) + b_D^{(l)}), \quad (11)$$

with $W_D^{(l)} \in \mathbb{R}^{D \times D}$, $b_D^{(l)} \in \mathbb{R}^D$, $W_C^{(l)} \in \mathbb{R}^{C \times C}$ and $b_C^{(l)} \in \mathbb{R}^C$. We use Z^+ from Equation (9) as the input for the first mixer block ($Z^0 = Z^+$). Figure 3 summarizes the architecture of the mixer blocks as introduced in this subsection.

4.5 Decoder

To obtain the forecasts we need to map the hidden state of each channel to the queries and decode it into a scalar for each pair of channel and query. Predicting continuous queries from fixed-sized vectors that represent a complete channel is not a novel problem and has been previously solved by concatenating the time stamp to the hidden state. The final prediction can then be inferred by a neural network [32].

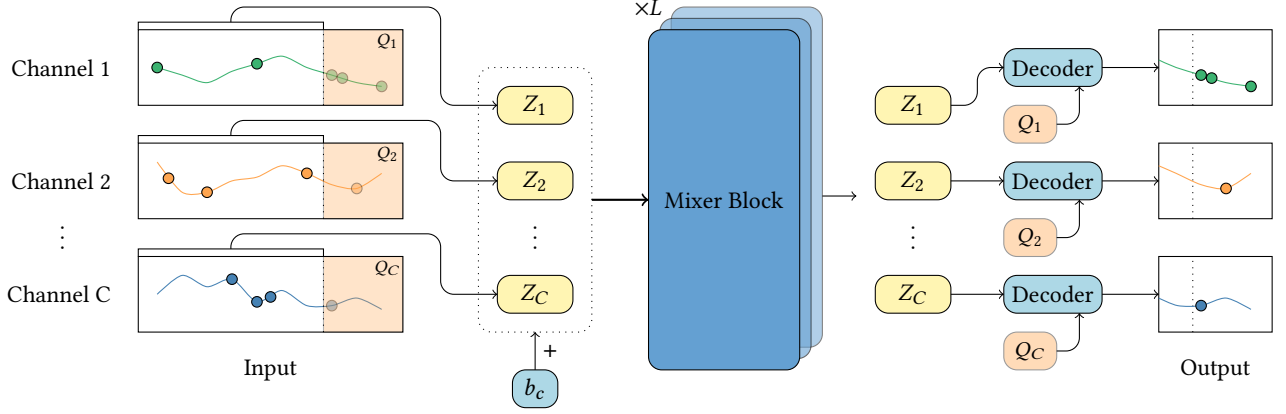


Figure 4: Overview of IMTS-Mixer's architecture

However, we propose an alternative method, that closely relates to how we computed the embeddings for observation-tuples, but is reversely applied. We input the query time as a scalar into a 2-layer neural network with D_{out} output neurons. The vector encoding of the query time is then multiplied element-wisely with the channel encoding and fed into linear layer that aggregates the vector product into a scalar. Formally, we obtain the prediction \hat{y} of channel c at query time $q_{i,c}$ with:

$$q_{i,c}^{enc} = W_2^q \text{relu}(W_1^q q_{i,c} + b_{c,1}^q) + b_{c,2}^q \quad (12)$$

$$\hat{y}_{i,c} = W^{out}(q_{i,c}^{enc} \odot Z_c^L) + b^{out} \quad (13)$$

4.6 Sharing weights

The modules for channel aggregation can either be shared across channels or kept separate for each channel. Sharing these modules reduces the number of parameters by a factor of C , though at the cost of some modeling flexibility.

Theoretically, a model must learn that a given set of observation tuples can have different implications depending on the channel. When channel aggregation and decoder weights are shared across channels, the model's ability to differentiate between channels is limited to the mixer blocks. However, this weight-sharing approach not only enhances parameter efficiency but also increases robustness against overfitting.

Based on our ablation studies, we found that the trade-off between expressiveness and robustness favors weight-sharing, at least within the evaluated setting. Since, the channels within one dataset can already be very different, we could theoretically train these modules over different datasets enabling a form of transfer learning. We do not share the weights of IMTS-Mixer's decoder.

5 Experiments

We conduct our experiments on an NVIDIA 3080TI with 12 GB of GPU Memory. We used the benchmark introduced by Zhang et al. [32], because it includes a wide range of baselines that are evaluated on various datasets and tasks.

5.1 Datasets

PhysioNet [19] and **MIMIC** [11] both contain vital signs of intensive care unit patients. To evaluate the models we query them to forecast all the measured variables for 24 hours based on all observations from the initial 24 hours after a patient's admission.

Human Activity [22] contains 3-dimensional positional records of four sensors attached resulting in 12 variables. The sensors are attached to individuals, which perform various activities (walking, sitting among others). Models are tasked to predict 1 second of human motion based on 3 seconds of observation.

Finally, **USHCN** [14] is created by combining daily meteorological measurements from over one thousand weather stations that are distributed over the US. While the 3 datasets mentioned above contain sparsely sampled IMTS intrinsically, USHCN originally is observed regularly and transformed into IMTS by randomly sampling observations. In each IMTS we use the 2 years of observations to predict the climate conditions of a single month. For each dataset we split the samples into 60% train 20% validation and 20% test data. Additional information about the datasets are given in Table 2.

Previous works [1, 5, 17, 27] used the parts of these datasets, but with different preprocessing, chunking and validation protocols. We want to emphasize that therefore, the results reported in these works are incomparable.

5.2 Hyperparameters

Following Yalavarthi et al. [27], we sample 10 hyperparameter configurations and select the one with the lowest MSE on the validation split. We tune the number of mixer-blocks, the dimension of the observation tuple embeddings and channel aggregation (D), as well as the output dimension of the final mixer block (D^{out}). The ranges are given in Appendix A.1. Furthermore, we set the hidden dimension of the non-linear networks that encode observation and query time stamps to 32. To train IMTS-Mixer, we implement the schedule-free AdamW[6, 12] optimizer with an initial learning rate of 0.01 and a weight decay of $1e-4$ while using early stopping with a patience of 10 epochs. Following Zhang et al. we use a batch-size of 32 for PhysioNet, MIMIC and Human Activity and a larger batch size of 128 for USHCN.

Table 1: Comparison of different algorithms across four datasets based on Test MSE and MAE. † indicates that results are reported from Zhang et al. [32]. Only tPatchGNN, GraFITi and IMTS-Mixer use tuned hyperparameters. For tPatchGNN we report both our own results as well the (untuned) results from Zhang et al. For the comparison, we focus on our own results, which is why the previously reported performance of tPatchGNN is in small font and parentheses. The best model is highlighted in bold and the second best is underlined.

Algorithm	PhysioNet		MIMIC		Human Activity		USHCN	
	MSE $\times 10^{-3}$	MAE $\times 10^{-2}$	MSE $\times 10^{-2}$	MAE $\times 10^{-2}$	MSE $\times 10^{-3}$	MAE $\times 10^{-2}$	MSE $\times 10^{-1}$	MAE $\times 10^{-1}$
DLinear [†]	41.86 \pm 0.05	15.52 \pm 0.03	4.90 \pm 0.00	16.29 \pm 0.05	4.03 \pm 0.01	4.21 \pm 0.01	6.21 \pm 0.00	3.88 \pm 0.02
TimesNet [†]	16.48 \pm 0.11	6.14 \pm 0.03	5.88 \pm 0.08	13.62 \pm 0.07	3.12 \pm 0.01	3.56 \pm 0.02	5.58 \pm 0.05	3.60 \pm 0.04
PatchTST [†]	12.00 \pm 0.23	6.02 \pm 0.14	3.78 \pm 0.03	12.43 \pm 0.10	4.29 \pm 0.14	4.80 \pm 0.09	5.75 \pm 0.01	3.57 \pm 0.02
Crossformer [†]	6.66 \pm 0.11	4.81 \pm 0.11	2.65 \pm 0.10	9.56 \pm 0.29	4.29 \pm 0.20	4.89 \pm 0.17	5.25 \pm 0.04	3.27 \pm 0.09
Graph Wavenet [†]	6.04 \pm 0.28	4.41 \pm 0.11	2.93 \pm 0.09	10.50 \pm 0.15	2.89 \pm 0.03	3.40 \pm 0.05	5.29 \pm 0.04	3.16 \pm 0.09
MTGNN [†]	6.26 \pm 0.18	4.46 \pm 0.07	2.71 \pm 0.23	9.55 \pm 0.65	3.03 \pm 0.03	3.53 \pm 0.03	5.39 \pm 0.05	3.34 \pm 0.02
StemGNN [†]	6.86 \pm 0.28	4.76 \pm 0.19	1.73 \pm 0.02	7.71 \pm 0.11	8.81 \pm 0.37	6.90 \pm 0.02	5.75 \pm 0.09	3.40 \pm 0.09
CrossGNN [†]	7.22 \pm 0.36	4.96 \pm 0.12	2.95 \pm 0.16	10.82 \pm 0.21	3.03 \pm 0.10	3.48 \pm 0.08	5.66 \pm 0.04	3.53 \pm 0.05
FourierGNN [†]	6.84 \pm 0.35	4.65 \pm 0.12	2.55 \pm 0.03	10.22 \pm 0.08	2.99 \pm 0.02	3.42 \pm 0.02	5.82 \pm 0.06	3.62 \pm 0.07
GRU-D [†]	5.59 \pm 0.09	4.08 \pm 0.05	1.76 \pm 0.03	7.53 \pm 0.09	2.94 \pm 0.05	3.53 \pm 0.06	5.54 \pm 0.38	3.40 \pm 0.28
SeFT [†]	9.22 \pm 0.18	5.40 \pm 0.08	1.87 \pm 0.01	7.84 \pm 0.08	12.20 \pm 0.17	8.43 \pm 0.07	5.80 \pm 0.19	3.70 \pm 0.11
RainDrop [†]	9.82 \pm 0.08	5.57 \pm 0.06	1.99 \pm 0.03	8.27 \pm 0.07	14.92 \pm 0.14	9.45 \pm 0.05	5.78 \pm 0.22	3.67 \pm 0.17
Warpformer [†]	5.94 \pm 0.35	4.21 \pm 0.12	1.73 \pm 0.04	7.58 \pm 0.13	2.79 \pm 0.04	3.39 \pm 0.03	5.25 \pm 0.05	3.23 \pm 0.05
mTAND [†]	6.23 \pm 0.24	4.51 \pm 0.17	1.85 \pm 0.06	7.73 \pm 0.13	3.22 \pm 0.07	3.81 \pm 0.07	5.33 \pm 0.05	3.26 \pm 0.10
Latent-ODE [†]	6.05 \pm 0.57	4.23 \pm 0.26	1.89 \pm 0.19	8.11 \pm 0.52	3.34 \pm 0.11	3.94 \pm 0.12	5.62 \pm 0.03	3.60 \pm 0.12
CRU [†]	8.56 \pm 0.26	5.16 \pm 0.09	1.97 \pm 0.02	7.93 \pm 0.19	6.97 \pm 0.78	6.30 \pm 0.47	6.09 \pm 0.17	3.54 \pm 0.18
Neural Flow [†]	7.20 \pm 0.07	4.67 \pm 0.04	1.87 \pm 0.05	8.03 \pm 0.19	4.05 \pm 0.13	4.46 \pm 0.09	5.35 \pm 0.05	3.25 \pm 0.05
(tPatchGNN [†])	(4.98 \pm 0.08)	(3.72 \pm 0.03)	(1.69 \pm 0.03)	(7.22 \pm 0.09)	(2.66 \pm 0.03)	(3.15 \pm 0.02)	(5.00 \pm 0.04)	(3.08 \pm 0.04)
tPatchGNN	5.44 \pm 0.14	3.85 \pm 0.24	1.33 \pm 0.02	6.58 \pm 0.11	2.70 \pm 0.06	3.18 \pm 0.06	<u>5.06 \pm 0.02</u>	<u>3.11 \pm 0.05</u>
GraFITi	4.91 \pm 0.05	<u>3.57 \pm 0.03</u>	1.21 \pm 0.01	6.19 \pm 0.07	<u>2.64 \pm 0.05</u>	<u>3.08 \pm 0.01</u>	5.17 \pm 0.07	3.19 \pm 0.19
IMTS-Mixer (ours)	4.88 \pm 0.03	3.47 \pm 0.01	<u>1.25 \pm 0.02</u>	<u>6.20 \pm 0.05</u>	2.49 \pm 0.01	3.06 \pm 0.01	5.01 \pm 0.08	3.05 \pm 0.03

Table 2: Summary of dataset characteristics. Obs. / Forc. Range refers to the observation range and forecasting horizon. Instances are the IMTS from training- validation- and test set combined. Channels are the number of variables observed. min/max avg. Obs. refers to the minimum/maximum number of observation per channel averaged over instances.

	PhysioNet	MIMIC	H. Activity	USHCN
Obs. / Forc. range	24h/24h	24h/24h	3s/1s	2y/1m
Instances	12,000	23,457	5,400	26,736
Channels	41	96	12	5
min avg. Obs.	0.07	0.0007	19.7	32.7
max avg. Obs.	31.1	3.3	23.9	35.6

5.3 Baselines

The baseline models from our main performance comparison are models not only from the IMTS forecasting literature, but also from RMTS forecasting and IMTS classification.

DLinear [29], TimesNet [23], PatchTST [15], Crossformer [34] Graph Wavenet [26], MTGNN [25], CrossGNN [10] and FourierGNN [28] are state-of-the-art models for RMTS Forecasting. GRU-D [2], SeFT [9], Raindrop [33], Warpformer [31] and mTAND [18]

are all models primarily introduced for IMTS classification, that are equipped with a predictor network which inputs hidden IMTS representations and query times.

Finally, Latent-ODE [16], Continuous Recurrent Units (CRU) [17], Neural Flow [1], tPatchGNN [32] and GraFITi [27] are models designed for IMTS Forecasting.

GraFITi has not been evaluated on Zhang et al.’s benchmark, and we contribute to the field of IMTS forecasting by running these experiments. In Appendix A.2, we list GraFITi’s hyperparameter space as mentioned in the corresponding paper [27]. We apply the random search protocol with 10 tries as explained above.

Following the same protocol and for the sake of a fair comparison, we also tune tPatchGNN, because it is the strongest method that was already contained in the benchmark. The hyperparameter ranges are build closely around the parameters that were reported by Zhang et al. and are listed in Appendix A.3.

For the remaining baselines, we report results directly from Zhang et al.. We refer to them for details including hyperparameters and the implemented strategies to evaluate RMTS Forecasting and IMTS classification models for IMTS forecasting.

5.4 Main Results

Table 1 reports the forecasting accuracy of IMTS-Mixer and GraFITi from our experiments as well as the baselines as given by Zhang et al. [32]. While all models were trained on Mean Squared Error (MSE) we also report the test Mean Absolute Error (MAE). The triplet of tPatchGNN, GraFITi, and IMTS-Mixer collectively represents the state-of-the-art as these models consistently achieve the top three performances across all datasets and metrics, while their relative rankings vary.

The MSE is the more relevant evaluation metric as models were optimized for it. Here, IMTS-Mixer performs best on PhysioNet, Activity and USHCN. However on PhysioNet, GraFITi is within the standard deviation and tPatchGNN is within the standard deviation on USHCN. On MIMIC, IMTS-Mixer shows to have the second-strongest performance being just slightly worse than GraFITi.

Comparing the MAE of competing models, we observe that IMTS-Mixer is even stronger than on MSE. On MAE, IMTS-Mixer is significantly better on PhysioNet, Human Activity and USHCN than the second-best model on each dataset. While GraFITi is still slightly better on MIMIC, the difference is insignificant.

The average ranks with respect to MSE and MAE are reported as 1.25 for IMTS-Mixer, 2 for GraFITi and 2.75 for tPatchGNN. We compute the average ranks exclusively based on the mean and ignore standard deviations.

Notably, the results of tPatchGNN vary significantly from the results that were reported by Zhang et al. [32]. While we expected them to be slightly better, because of tuning, the test errors are actually higher for three out of four tasks. However, we verified that the hyperparameter configurations that we chose performed best on the respective validation data. In their paper, Zhang et al., show experiments with different values for the hyperparameter *Patch-Size* and select the configuration that performs best on the test set, which is a form of tuning on test data.

While the comparison to the non-tuned baselines is difficult, the evaluation between IMTS-Mixer, GraFITi and tPatchGNN is definitely fair.

5.5 Efficiency Analysis

In Figure 5, we show the inference and training time per epoch of each model that we trained. We refer to the hyperparameter configurations that were tuned based on validation MSE. The training time per epoch represents the time a model takes on our setup to predict the queries, compute the loss-gradient and update its weights for all mini-batches contained in the training data. The inference time refers to the total time it takes to answer all queries from the test set. We observe that IMTS-Mixer’s inference time is consistently shorter than the inference time of GraFITi and tPatchGNN. Furthermore, it has the fastest training time per epoch on all datasets but MIMIC, where it is slightly slower than GraFITi. On MIMIC, the tuning results in the largest and slowest hyperparameter configuration that we made available for IMTS-Mixer. Hence, we could obtain a significantly faster model with slightly worse forecasting accuracy.

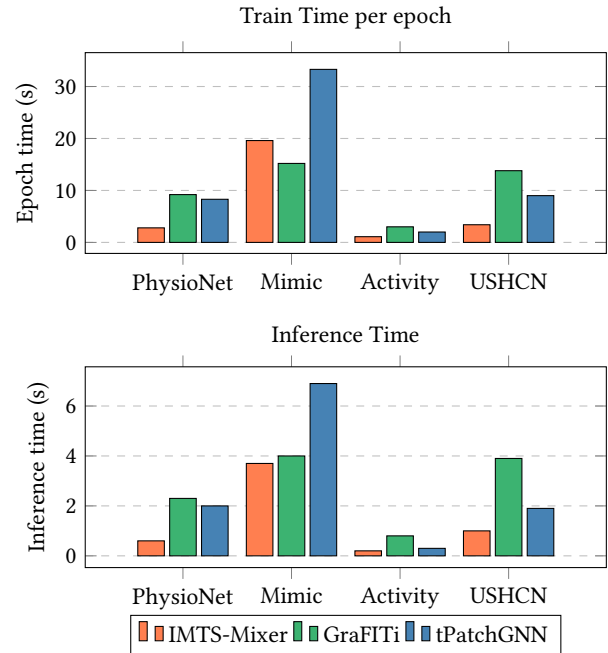


Figure 5: Training and inference time in seconds. We refer to the hyperparameters corresponding to the results shown in Table 1.

6 Ablations

We conduct a series of ablation experiments to evaluate the impact of each model component included in IMTS-Mixer. The results are summarized Table 3.

6.1 Mixer-Blocks

In a first experiment we leave out the mixer blocks. Hence, our decoder is directly applied to the result of the channel aggregation. As expected, IMTS-Mixer performs significantly better with mixer blocks than without them, because the mixer blocks are the only modules in our architecture capable of modeling channel interactions. However, our mixer-less ablation (*w/o Mixer Blocks*) still outperforms several competing models presented in Table 1, including CRU, Latent-ODE, and Neural Flow, and even surpasses tPatchGNN on some datasets, calling the usefulness of these baselines into question.

We also want to investigate, if applying a mixer network is actually necessary. Alternatively, we could replace the mixer blocks with wide fully connected layers $CD \rightarrow CD$ combined with relu activation. The respective model is named *FC-Mixer*. We observe that its performance is significantly worse justifying the mixer blocks as implemented for IMTS-Mixer.

6.2 Channel aggregation with mTAN

As we mentioned in Section 2.2.3, the mTAN [18] module imputes a time series at predefined equally spaced reference points. Concatenated, the scalar imputations of these reference points can be interpreted as vectors, where one vector represents one channel. In

Table 3: Test MSE and MAE of Ablations

Algorithm	PhysioNet		MIMIC		Human Activity		USHCN	
	MSE $\times 10^{-3}$	MAE $\times 10^{-2}$	MSE $\times 10^{-2}$	MAE $\times 10^{-2}$	MSE $\times 10^{-3}$	MAE $\times 10^{-2}$	MSE $\times 10^{-1}$	MAE $\times 10^{-1}$
IMTS-Mixer	4.88 \pm 0.03	3.47 \pm 0.01	1.25 \pm 0.02	6.20 \pm 0.05	2.49 \pm 0.01	3.06 \pm 0.01	5.01 \pm 0.08	3.05 \pm 0.03
w/o Mixer Blocks	5.17 \pm 0.03	3.55 \pm 0.01	1.36 \pm 0.02	6.57 \pm 0.06	2.74 \pm 0.01	3.16 \pm 0.01	5.14 \pm 0.04	3.07 \pm 0.03
FC-Mixer	4.94 \pm 0.04	3.52 \pm 0.03	1.31 \pm 0.01	6.43 \pm 0.04	2.64 \pm 0.02	3.21 \pm 0.01	5.15 \pm 0.07	3.15 \pm 0.05
w/o Value Emb.	5.25 \pm 0.07	3.52 \pm 0.01	1.36 \pm 0.03	6.67 \pm 0.13	2.48 \pm 0.01	3.04 \pm 0.01	5.07 \pm 0.07	3.10 \pm 0.03
w/o Weight-Sharing	5.06 \pm 0.10	3.47 \pm 0.01	1.25 \pm 0.01	6.20 \pm 0.03	2.51 \pm 0.01	3.09 \pm 0.01	5.09 \pm 0.09	3.11 \pm 0.05
w/o Channel Bias	4.95 \pm 0.13	3.50 \pm 0.03	1.28 \pm 0.02	6.30 \pm 0.02	2.54 \pm 0.02	3.10 \pm 0.01	5.19 \pm 0.01	3.10 \pm 0.01
mTAN-Mixer	6.65 \pm 0.06	5.07 \pm 0.01	1.94 \pm 0.03	9.82 \pm 0.01	2.61 \pm 0.07	3.16 \pm 0.05	5.39 \pm 0.10	3.32 \pm 0.05

the full mTAND architecture, the mTAN module is used not only for IMTS encoding, but additionally it is used to interpolate IMTS observations based on a fixed-sized hidden state. Hence, we can construct an ablation that works without the channel aggregation and decoder that we introduced replacing these modules with mTAN. That model imputes reference points with mTAN, applies mixer-blocks and infers the final prediction using the mTAN module in the same way it is used for interpolation. We name the resulting model *mTAN-Mixer*. As shown in Table 3, it has a significantly worse performance than IMTS-Mixer, while providing a lower test MSE and MAE than numerous baseline models. These results show that the channel aggregation introduced by us is better than mTAN.

6.3 Initial Value Encoding

As described in Section 4.1, we first transform the scalar value into a vector (v^{enc}), that is then used to compute the observation tuple embedding and the respective weight necessary for the channel aggregation. To evaluate, if this initial linear layer is actually useful, we conduct an ablation study that replaces this initial linear layer with the identity function. Hence, v_i^{enc} is replaced by a vector of the same size with the scalar v_i at every index. We list the resulting model under the name *w/o Value Emb.* in Table 3. We observe that the linear value embedding has a significant positive impact on all datasets but Human Activity, where it has a minimal negative impact.

6.4 Sharing Weights

We perform experiments to evaluate the impact of channel-wise weight-sharing for the channel aggregation. The results, presented under *w/o weight-sharing*, demonstrate that the increased robustness provided by weight-sharing outweighs its reduced expressiveness. Sharing the weights, yields in a slightly lower Test-MSE.

6.5 Channel Bias

As a final ablation study, we investigate the usefulness of the learnable channel bias added to the channel encoding of IMTS-Mixer. The results, shown in the line *w/o Channel Bias*, indicate that the channel bias has a positive impact on both MSE and MAE for all four datasets.

7 Limitations

Theoretically, IMTS-Mixer is limited by its fixed-size channel aggregation, which aggregates the sequence of observations from a channel into a fixed-sized embedding. For really long sequences or if there exist significant differences in typical sequence lengths across channels, the fixed representation may become a bottleneck or struggle to represent the significantly different channels in a unified fashion.

However, in practice, we do not find this to be an issue. Our model is able to fit all the common benchmark datasets well with varying number of channels and distribution of sequence lengths. We also saw in an ablation study in Table 3 that not sharing the weights between channels in the initial encoding is worse for all datasets. So even with shared weights, the model is able to learn meaningful representations for channels of different types or lengths.

Another potential limitation is that the mixer blocks currently scale quadratically with the number of channels. In our experiments this is not a practical issue, however, and for modelling datasets with orders of magnitudes more channels than we currently consider, it would be possible to extend the model to reduce the number of channels before the mixer blocks.

8 Conclusion and Future Work

We introduced IMTS-Mixer, the first TS mixer architecture for IMTS forecasting. The key innovation lies in its channel aggregation and decoding mechanism, which enables the use of fully connected layers on irregularly observed channels. Our ablation studies demonstrate that embedding and aggregation modules can be shared across channels, allowing for a universal transformation from irregularly observed data to fixed-sized vectors.

Our experiments show that IMTS-Mixer outperforms competing methods on three out of four benchmark datasets. Moreover, on the fourth dataset (MIMIC), our experiment established a new state-of-the-art with GraFITi, while our model performs second best. Additionally, our architecture achieves a speed-up in training and inference time.

For future work, we aim to explore how certain modules introduced in IMTS-Mixer can benefit other forecasting models.

References

- [1] Marin Biloš, Johanna Sommer, Syama Sundar Rangapuram, Tim Januschowski, and Stephan Günemann. 2021. Neural Flows: Efficient Alternative to Neural ODEs. In *Advances in Neural Information Processing Systems*, Vol. 34. Curran Associates, Inc., 21325–21337.
- [2] Zhengping Che, Sanjay Purushotham, Kyunghyun Cho, David Sontag, and Yan Liu. 2018. Recurrent Neural Networks for Multivariate Time Series with Missing Values. *Scientific Reports* 8, 1 (April 2018), 6085. doi:10.1038/s41598-018-24271-9
- [3] Ricky T. Q. Chen, Yulia Rubanova, Jesse Bettencourt, and David K Duvenaud. 2018. Neural Ordinary Differential Equations. In *Advances in Neural Information Processing Systems*, Vol. 31. Curran Associates, Inc.
- [4] Si-An Chen, Chun-Liang Li, Sercan O. Arik, Nathanael Christian Yoder, and Tomas Pfister. 2023. TSMixer: An All-MLP Architecture for Time Series Forecasting. (2023).
- [5] Edward De Brouwer, Jaak Simm, Adam Arany, and Yves Moreau. 2019. GRU-ODE-Bayes: Continuous Modeling of Sporadically-Observed Time Series. In *Advances in Neural Information Processing Systems*, Vol. 32. Curran Associates, Inc.
- [6] Aaron Defazio, Xingyu Alice Yang, Harsh Mehta, Konstantin Mishchenko, Ahmed Khaled, and Ashok Cutkosky. 2024. The Road Less Scheduled. doi:10.48550/arXiv.2405.15682 arXiv:2405.15682 [cs]
- [7] Vijay Ekambaram, Arindam Jati, Nam Nguyen, Phanwadee Sinthong, and Jayant Kalagnanam. 2023. TSMixer: Lightweight MLP-Mixer Model for Multivariate Time Series Forecasting. In *Proceedings of the 29th ACM SIGKDD Conference on Knowledge Discovery and Data Mining* (New York, NY, USA, 2023-08-04) (*KDD '23*). Association for Computing Machinery, 459–469. doi:10.1145/3580305.3599533
- [8] Kaiming He, Xiangyu Zhang, Shaoqing Ren, and Jian Sun. 2016. Deep Residual Learning for Image Recognition. In *2016 IEEE Conference on Computer Vision and Pattern Recognition (CVPR)*. IEEE, Las Vegas, NV, USA, 770–778. doi:10.1109/CVPR.2016.90
- [9] Max Horn, Michael Moor, Christian Bock, Bastian Rieck, and Karsten Borgwardt. 2020. Set Functions for Time Series. In *Proceedings of the 37th International Conference on Machine Learning*. PMLR, 4353–4363.
- [10] Qihe Huang, Lei Shen, Ruixun Zhang, Shouhong Ding, Binwu Wang, Zhengyang Zhou, and Yang Wang. 2023. CrossGNN: Confronting Noisy Multivariate Time Series Via Cross Interaction Refinement. *Advances in Neural Information Processing Systems* 36 (Dec. 2023), 46885–46902.
- [11] Alistair E. W. Johnson, Tom J. Pollard, Lu Shen, Li-wei H. Lehman, Mengling Feng, Mohammad Ghassemi, Benjamin Moody, Peter Szolovits, Leo Anthony Celi, and Roger G. Mark. 2016. MIMIC-III, a Freely Accessible Critical Care Database. *Scientific Data* 3, 1 (May 2016), 160035. doi:10.1038/sdata.2016.35
- [12] Diederik P. Kingma and Jimmy Ba. 2017. Adam: A Method for Stochastic Optimization. doi:10.48550/arXiv.1412.6980 arXiv:1412.6980 [cs]
- [13] Yong Liu, Tengge Hu, Haoran Zhang, Haixu Wu, Shiyu Wang, Lintao Ma, and Mingsheng Long. 2023. iTransformer: Inverted Transformers Are Effective for Time Series Forecasting. In *The Twelfth International Conference on Learning Representations*.
- [14] M. J. Menne, Jr Williams, and R. S. Vose. 2006. *U.S. HISTORICAL CLIMATOLOGY NETWORK (USHCN): Daily Temperature, Precipitation, and Snow Data*. Technical Report. Environmental System Science Data Infrastructure for a Virtual Ecosystem (ESS-DIVE) (United States); Carbon Dioxide Information Analysis Center (CDIAC), Oak Ridge National Laboratory (ORNL), Oak Ridge, TN (United States). doi:10.3334/CDIAC/CLINDP070
- [15] Yuqi Nie, Nam H. Nguyen, Phanwadee Sinthong, and Jayant Kalagnanam. 2022. A Time Series Is Worth 64 Words: Long-term Forecasting with Transformers. In *The Eleventh International Conference on Learning Representations*.
- [16] Yulia Rubanova, Ricky T. Q. Chen, and David K Duvenaud. 2019. Latent Ordinary Differential Equations for Irregularly-Sampled Time Series. In *Advances in Neural Information Processing Systems*, Vol. 32. Curran Associates, Inc.
- [17] Mona Schirmer, Mazin Eltayeb, Stefan Lessmann, and Maja Rudolph. 2022. Modeling Irregular Time Series with Continuous Recurrent Units. In *Proceedings of the 39th International Conference on Machine Learning*. PMLR, 19388–19405.
- [18] Satya Narayan Shukla and Benjamin Marlin. 2020. Multi-Time Attention Networks for Irregularly Sampled Time Series. In *International Conference on Learning Representations*.
- [19] Ikaro Silva, George Moody, Daniel J Scott, Leo A Celi, and Roger G Mark. 2012. Predicting In-Hospital Mortality of ICU Patients: The PhysioNet/Computing in Cardiology Challenge 2012. In *2012 Computing in Cardiology*. 245–248.
- [20] Ilya O Tolstikhin, Neil Houlsby, Alexander Kolesnikov, Lucas Beyer, Xiaohua Zhai, Thomas Unterthiner, Jessica Yung, Andreas Steiner, Daniel Keysers, Jakob Uszkoreit, Mario Lucic, and Alexey Dosovitskiy. 2021. MLP-Mixer: An All-MLP Architecture for Vision. In *Advances in Neural Information Processing Systems*, Vol. 34. Curran Associates, Inc., 24261–24272.
- [21] Ashish Vaswani, Noam Shazeer, Niki Parmar, Jakob Uszkoreit, Llion Jones, Aidan N Gomez, Ł ukasz Kaiser, and Illia Polosukhin. 2017. Attention Is All You Need. In *Advances in Neural Information Processing Systems*, Vol. 30. Curran Associates, Inc.
- [22] Mitja Lustrek Vedrana Vidulin. 2010. Localization Data for Person Activity. doi:10.24432/C57G8X
- [23] Haixu Wu, Tengge Hu, Yong Liu, Hang Zhou, Jianmin Wang, and Mingsheng Long. 2022. TimesNet: Temporal 2D-Variation Modeling for General Time Series Analysis. In *The Eleventh International Conference on Learning Representations*.
- [24] Haixu Wu, Jiehui Xu, Jianmin Wang, and Mingsheng Long. 2021. Autoformer: Decomposition Transformers with Auto-Correlation for Long-Term Series Forecasting. In *Advances in Neural Information Processing Systems*, Vol. 34. Curran Associates, Inc., 22419–22430.
- [25] Zonghan Wu, Shirui Pan, Guodong Long, Jing Jiang, Xiaojun Chang, and Chengqi Zhang. 2020. Connecting the Dots: Multivariate Time Series Forecasting with Graph Neural Networks. In *Proceedings of the 26th ACM SIGKDD International Conference on Knowledge Discovery & Data Mining (KDD '20)*. Association for Computing Machinery, New York, NY, USA, 753–763. doi:10.1145/3394486.3403118
- [26] Zonghan Wu, Shirui Pan, Guodong Long, Jing Jiang, and Chengqi Zhang. 2019. Graph Wavenet for Deep Spatial-Temporal Graph Modeling. In *Proceedings of the 28th International Joint Conference on Artificial Intelligence (IJCAI'19)*. AAAI Press, Macao, China, 1907–1913.
- [27] Vijaya Krishna Yalavarthi, Kiran Madhusudhanan, Randolph Scholz, Nourhan Ahmed, Johannes Burchert, Shayan Jawed, Stefan Born, and Lars Schmidt-Thieme. 2024. GraFITi: Graphs for Forecasting Irregularly Sampled Time Series. *Proceedings of the AAAI Conference on Artificial Intelligence* 38, 15 (March 2024), 16255–16263. doi:10.1609/aaai.v38i15.29560
- [28] Kun Yi, Qi Zhang, Wei Fan, Hui He, Liang Hu, Pengyang Wang, Ning An, Longbing Cao, and Zhenqiang Niu. 2023. FourierGNN: Rethinking Multivariate Time Series Forecasting from a Pure Graph Perspective. *Advances in Neural Information Processing Systems* 36 (Dec. 2023), 69638–69660.
- [29] Ailing Zeng, Muxi Chen, Lei Zhang, and Qiang Xu. 2023. Are Transformers Effective for Time Series Forecasting? *Proceedings of the AAAI Conference on Artificial Intelligence* 37, 9 (June 2023), 11121–11128. doi:10.1609/aaai.v37i9.26317
- [30] Biao Zhang and Rico Sennrich. 2019. Root Mean Square Layer Normalization. In *Advances in Neural Information Processing Systems*, Vol. 32. Curran Associates, Inc.
- [31] Jiawen Zhang, Shun Zheng, Wei Cao, Jiang Bian, and Jia Li. 2023. Warpformer: A Multi-scale Modeling Approach for Irregular Clinical Time Series. In *Proceedings of the 29th ACM SIGKDD Conference on Knowledge Discovery and Data Mining (KDD '23)*. Association for Computing Machinery, New York, NY, USA, 3273–3285. doi:10.1145/3580305.3599543
- [32] Weijia Zhang, Chenlong Yin, Hao Liu, Xiaofang Zhou, and Hui Xiong. 2024. Irregular Multivariate Time Series Forecasting: A Transformable Patching Graph Neural Networks Approach. In *Forty-First International Conference on Machine Learning*.
- [33] Xiang Zhang, Marko Zeman, Theodoros Tsiligkaridis, and Marinka Zitnik. 2021. Graph-Guided Network for Irregularly Sampled Multivariate Time Series. In *International Conference on Learning Representations*.
- [34] Yunhao Zhang and Junchi Yan. 2022. Crossformer: Transformer Utilizing Cross-Dimension Dependency for Multivariate Time Series Forecasting. In *The Eleventh International Conference on Learning Representations*.
- [35] Haoyi Zhou, Shanghang Zhang, Jieqi Peng, Shuai Zhang, Jianxin Li, Hui Xiong, and Wancai Zhang. 2021. Informer: Beyond Efficient Transformer for Long Sequence Time-Series Forecasting. *Proceedings of the AAAI Conference on Artificial Intelligence* 35, 12 (May 2021), 11106–11115. doi:10.1609/aaai.v35i12.17325
- [36] Tian Zhou, Ziqing Ma, Qingsong Wen, Xue Wang, Liang Sun, and Rong Jin. 2022. FEDformer: Frequency Enhanced Decomposed Transformer for Long-term Series Forecasting. In *Proceedings of the 39th International Conference on Machine Learning*. PMLR, 27268–27286.

A Hyperparameters

A.1 IMTS-Mixer

- We tune the dimension of the aggregated channels D from the set $\{64, 128, 256\}$
- The range for D_{out} is $\{32, 64, 128\}$
- We allow the number of mixer blocks to be $\{1, 2, 3\}$

A.2 GraFITi

We use the hyperparameter ranges as given by Yalavarthi et al.:

- We tune the number of layers from $\{1, 2, 3, 4\}$
- The attention mechanism can use a number of heads from the set of $\{1, 2, 4\}$

- The latent dimension is sampled from $\{16, 32, 64, 128, 256\}$

A.3 tPatchGNN

The hyperparameters reported from Zhang et al. are highlighted in **bold**. As authors used different hyperparameters for each dataset most hyperparameters have multiple options marked in bold. We refer to original paper for additional details [32]

- The hidden dimension is selected from $\{32, 64, 128\}$
- The time embedding dimension is taken from $\{5, 10, 20\}$
- The patch size
 - is sampled from $\{2, 4, 8\}$ for PhysioNet, MIMIC, USHCN
 - is sampled from $\{100, 300, 750\}$ for Activity